

A discrete-sectional model for particle growth in aerosol reactor: Application to titania particles

Chowdhury Golam Moniruzzaman and Kyun Young Park[†]

Department of Chemical Engineering, Kongju National University, Gongju, Chungnam 314-701, Korea
(Received 10 July 2005 • accepted 8 September 2005)

Abstract—A one-dimensional discrete-sectional model has been developed to simulate particle growth in aerosol reactors. Two sets of differential equations for volume and surface area, respectively, were solved simultaneously to determine the size distributions of agglomerates and primary particles. The surface area equations were derived in such a way that the coagulation integrals calculated for the volume equations could be used for the surface area equations as well, which is new in this model. The model was applied to a production of TiO₂ particles by oxidation of titanium tetrachloride. Model predictions were compared with experimental data and those of a two-dimensional sectional model. Good agreement was shown in calculated particle size distributions between the present model and the two-dimensional model, which is more rigorous but demands a large amount of computer time and memory. Compared to experimental data, the primary particle size calculated by the model was more sensitive to the variation of reactor temperature.

Key words: Coalescence, Coagulation, Primary Particle and Discrete-Sectional Model

INTRODUCTION

Aerosol reactors, in which small particles suspended in gases are formed by chemical reaction, have been used to produce a variety of particles for different applications. Carbon black, silica and titania are well-known examples. Initially, the aerosol precursor is converted by chemical reaction to condensable product molecules. The condensable molecules self-nucleate to form a cloud of stable nuclei that grow subsequently by collision to larger particles. The particle size distribution at a time can be represented by the general dynamic equation (GDE), in discrete or continuous form [Friedlander, 1977]. The discrete GDE, while rigorously valid, is impractical because of the huge demands on computer time and memory. The continuous GDE is more tractable but cannot represent the particle growth where discrete size effects are important.

A discrete-continuous model was proposed later; the discrete representation is used up to a certain size past which the particle size distribution is represented as continuous [Gelbard and Seinfeld, 1979]. The discrete-continuous model still requires an impractically large amount of computer time for a system in which the particle size varies over orders of magnitude. By dividing the continuous size domain into finite sections, the discrete-continuous model was extended to the discrete-sectional model that reduced the computational load considerably [Okuyama et al., 1986; Wu and Flagan, 1988; Landgrebe and Pratsinis, 1990]. In these discrete-sectional models, however, particles were assumed to coalesce instantaneously on collision to form spherical particles, although in aerosol reactors fractal-like agglomerates composed of many primary particles are often formed due to incomplete coalescence.

The concept of a finite rate of coalescence for neighboring primary particles comprising an agglomerate was first introduced by Koch and Friedlander [1990]. They proposed a simple law by which

the surface area of an agglomerate decreases with time by sintering, in proportion to the difference between instantaneous surface area and the area of the completely fused sphere of equal volume. Xiong and Pratsinis [1993a] incorporated the sintering law into a sectional model to study the growth of primary particles due to sintering. Their model was two-dimensional with particle volume and area as coordinates, and required enormous computation time to calculate the quadruple integrals for coagulation and sintering coefficients. Simpler one-dimensional sectional models comparable to the two dimensional model were reported later by Tsantilis and Pratsinis [2000] and Jeong and Choi [2001]. The two models differ in the method of approximating the particle size distribution in a section. In the model of Tsantilis and Pratsinis, a representative size was assumed for all the particles in a section, while in the model of Jeong and Choi, the size distribution was assumed to be constant at the mean value determined so that the number of particles in the section can be conserved. Two sets of differential equations were set up: one for the volume and the other for the surface area. By solving the equations simultaneously, the volume and the area of each section were obtained, from which average primary particle size in the section was determined. The problem with these sectional models is that the cluster dynamics cannot be properly taken into consideration.

In the present work, a one-dimensional discrete-sectional model was developed. The volume and area equations were used to determine primary particle size, as in the Jeong and Choi's sectional model. However, it is new in that the surface area equations were derived in a different way so that the coagulation integrals calculated for the volume equations could be used as well by the area equations, thereby reducing computation time and memory. Another difference is that the interactions between small discrete particles or molecular clusters and agglomerates were taken into account. The small clusters, on collision with an agglomerate, were assumed to coalesce instantaneously on the primary particles.

The present model was applied to a production of TiO₂ particles by oxidation of titanium tetrachloride. Model predictions were com-

[†]To whom correspondence should be addressed.
E-mail: kypark@kongju.ac.kr

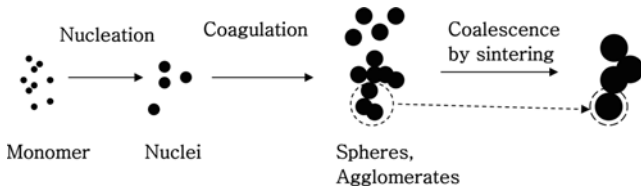


Fig. 1. Particle growth mechanism in aerosol reactors.

pared with experimental data and those by the two-dimensional model by Xiong and Pratsinis [1993b].

MODEL DERIVATION

Fig. 1 shows the generation and growth of particles by nucleation, coagulation and coalescence in an aerosol reactor. The rate of change of particle numbers with respect to time and particle size can be represented by the GDE also called as the Population Balance Equation (PBE) [Friedlander, 1977] as follows:

$$\frac{\partial n}{\partial t} + \frac{\partial(Gn)}{\partial v} - I(v^*)\delta(v - v^*) = \frac{1}{2} \int_0^v \beta(v-u, u)n(v-u, t)n(u, t)du - n(v, t) \int_0^{\infty} \beta(v, u)n(u, t)du \quad (1)$$

The first term of the left-hand side (LHS) is the rate of change of total number of particles in the particle volume from v to $v+dv$. The second LHS term is the loss or gain of number of particles by condensation at a rate G . The third LHS term is the rate of formation of new particles of critical volume v^* at a rate of I . The two right-hand-side (RHS) terms are the gain and loss of particles by coagulation, respectively, in the particle volume from v to $v+dv$.

By applying the discrete-sectional method to the GDE, the rate of change of volume and surface area of discrete particles or particles in a section can be represented as ordinary differential equations. The equations for volume are similar to those used in previous models, but the equations for surface area include our own idea to share the collision integrals calculated for the volume equations.

Fig. 2 illustrates the discrete and sectional regimes. In the discrete regime, particles are assumed to be spherical. In the sectional regime, the particles are either spherical or in agglomerated form depending on operating conditions. The agglomerates form if the temperature is not high enough for complete coalescence of particles on collision.

1. Volume Equations

The rate of change of total volume of monomers is represented by

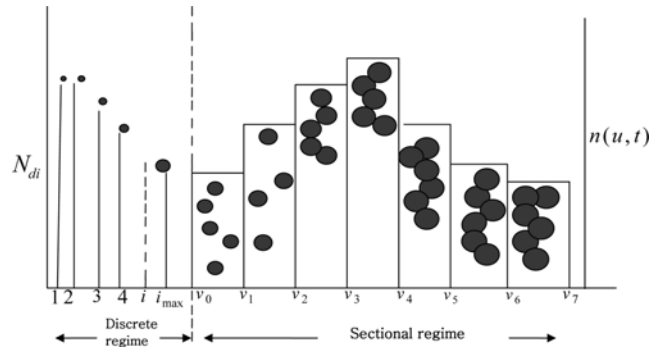


Fig. 2. Illustration of discrete and sectional regimes. N_{di} and $n(u, t)$ represent the number of i -mers per unit volume of gas in the discrete-regime and the number distribution function for particles of volume u in the sectional regime, respectively.

$$\frac{dV_{d1}}{dt} = Iv_m - V_{d1} \sum_{j=1}^{i_{max}} \beta_{1,j}^{2DD} V_{dj} - V_{d1} \sum_{k=1}^m \beta_{1,k}^{3DS} V_{sk} \quad (2)$$

where V_{d1} is the volume of monomers, I is the nucleation rate of monomer, v_m is the monomer volume, V_{dj} is the volume of j -mers (particles consisting of j molecules), $\beta_{1,j}^{2DD}$ is the coagulation coefficient for the monomers and the j -mers, V_{sk} is the volume of all the particles in the k^{th} section and $\beta_{1,k}^{3DS}$ is the coagulation integral for the monomers and the particles in the k^{th} section. It is shown in Tables 1, 2 and 3 how the coagulation coefficients for discrete particles and the coagulation integrals for agglomerates are calculated. The first RHS term of Eq. (2) is the generation rate of V_{d1} by nucleation. The second and third RHS terms account for the loss of V_{d1} by coagulation of monomers with all discrete particles and agglomerates in sections, respectively.

A product monomer was assumed to be a nucleus. This assumption has been used for materials like TiO_2 and SiO_2 whose vapor pressures are extremely low [Ulrich, 1971]. The nucleation rate, I , can be calculated by the equation, $I=k_p c^n$, where k_p is the rate constant, c is the concentration of precursor and n is the reaction order.

The population balance for the volume of i -mers, V_{di} , ($i=2$ to i_{max}) is

$$\frac{dV_{di}}{dt} = \frac{1}{2} \sum_{j=1}^{i-1} \beta_{j,i-j}^{1DD} V_{dj} V_{d(i-j)} - V_{di} \sum_{j=1}^{i_{max}} \beta_{i,j}^{2DD} V_{dj} - V_{di} \sum_{k=1}^m \beta_{i,k}^{3DS} V_{sk} \quad (3)$$

The first RHS term is the production rate of V_{di} by coagulation of smaller discrete particles, while the second and third RHS terms are the loss of V_{di} by coagulation of i -mers with all discrete particles and agglomerates in sections, respectively.

Table 1. Discrete-discrete coagulation coefficients

$\beta_{j,i-j}^{1DD}$	$\frac{\beta\{jv_m, (i-j)v_m\} [iv_m]}{(jv_m)\{(i-j)v_m\}}$	$[2 \leq i \leq i_{max}] [1 \leq j \leq i-1]$
	Coefficient for coagulation of a j -mer and a $(i-j)$ -mer to produce i -mer.	
β_{ij}^{2DD}	$\frac{\beta(iv_m, jv_m)}{(jv_m)}$	$[1 \leq i \leq i_{max}] [1 \leq j \leq i_{max}]$
	Coefficient for coagulation of a i -mer and a j -mer.	
$\beta_{i,j,k}^{3DD}$	$\frac{\theta[v_{k-1} \leq iv_m + jv_m \leq v_k] \beta(iv_m, jv_m)}{(iv_m)(jv_m)}$	$[1 \leq i \leq i_{max}] [1 \leq j \leq i_{max}] [1 \leq k \leq m]$
	Coefficient for coagulation of an i -mer and a j -mer to produce an agglomerate in the k^{th} section.	

Table 2. Section-Section coagulation integrals

$\beta_{i,j,k}^{1SS}$	$\int_{v_{j-1}}^{v_j} \int_{v_{j-1}}^{v_j} \frac{\theta[v_{k-1} < u + v < v_k] \beta(u, v) (u + v) dv du}{u v (v_j - v_{j-1}) (v_j - v_{j-1})}$	
$\beta_{i,j,k}^{1SS1}$	$\int_{v_{j-1}}^{v_j} \int_{v_{j-1}}^{v_j} \frac{\theta[v_{k-1} < u + v < v_k] \beta(u, v) dv du}{v (v_j - v_{j-1}) (v_j - v_{j-1})}$	
$\beta_{i,j,k}^{1SS2}$	$\int_{v_{j-1}}^{v_j} \int_{v_{j-1}}^{v_j} \frac{\theta[v_{k-1} < u + v < v_k] \beta(u, v) dv du}{u (v_j - v_{j-1}) (v_j - v_{j-1})}$	
	$\beta_{i,j,k}^{1SS} = \beta_{i,j,k}^{1SS1} + \beta_{i,j,k}^{1SS2}$	$[1 \leq i \leq k-1] [1 \leq j \leq k-1] [2 \leq k \leq m]$
	Coagulation integral for an agglomerate produced in the k^{th} section by coagulation of two smaller section agglomerates, one in the i^{th} section and the other in the j^{th} section.	
$\beta_{i,k}^{2SS}$	$\int_{v_{i-1}}^{v_i} \int_{v_{k-1}}^{v_k} \frac{\theta[u + v > v_k] \beta(u, v) dv du}{u (v_i - v_{i-1}) (v_k - v_{k-1})}$	$[1 \leq i \leq k-1] [2 \leq k \leq m]$
	Coagulation integral for an agglomerate removed from the k^{th} section by coagulation of a k^{th} section agglomerate and a smaller i^{th} section agglomerate.	
β_k^{3SS}	$\int_{v_{k-1}}^{v_k} \int_{v_{k-1}}^{v_k} \frac{\theta[u + v > v_k] \beta(u, v) (u + v) dv du}{u v (v_k - v_{k-1})^2}$	$[1 \leq k \leq m]$
	Coagulation integral for an agglomerate removed from the k^{th} section by coagulation of two k^{th} section agglomerates.	
$\beta_{i,k}^{4SS}$	$\int_{v_{i-1}}^{v_i} \int_{v_{k-1}}^{v_k} \frac{\beta(u, v)}{u (v_i - v_{i-1}) (v_k - v_{k-1})} dv du$	$[k+1 \leq i \leq m] [1 \leq k \leq m]$
	Coagulation integral for an agglomerate removed from the k^{th} section by coagulation of a k^{th} section agglomerate and a bigger i^{th} section agglomerate.	
$\beta_{i,k}^{5SS}$	$\int_{v_{i-1}}^{v_i} \int_{v_{k-1}}^{v_k} \frac{\theta[u + v < v_k] \beta(u, v) dv du}{v (v_i - v_{i-1}) (v_k - v_{k-1})}$	$[1 \leq i \leq k-1] [2 \leq k \leq m]$
	Coagulation integral for an agglomerate produced in the k^{th} section by coagulation of a k^{th} section agglomerate and a smaller i^{th} section agglomerate.	

Table 3. Discrete-section coagulation integrals

V_{sk}	$\int_{v_{j-1}}^{v_k} \frac{\theta[v_{k-1} < i v_m + u < v_k] \beta(i v_m, u) (1 + i v_m / u)^{2/3}}{(i v_m) (v_j - v_{j-1})} du$	$[1 \leq i \leq i_{max}] [1 \leq j \leq k-1] [2 \leq k \leq m]$
	Coagulation integral for an agglomerate produced in the k^{th} section by coagulation of a smaller j^{th} section agglomerate and an i -mer.	
$\beta_{i,k}^{2DS}$	$\int_{v_{i-1}}^{v_k} \frac{\theta[i v_m + u > v_k] \beta(i v_m, u) du}{i v_m (v_k - v_{k-1})}$	$[1 \leq i \leq i_{max}] [1 \leq k \leq m]$
	Coagulation integral for an agglomerate removed from the k^{th} section by coagulation of a k^{th} section agglomerate and an i -mer.	
$\beta_{i,k}^{3DS}$	$\int_{v_{i-1}}^{v_k} \frac{\beta(i v_m, u) du}{u (v_k - v_{k-1})}$	$[1 \leq i \leq i_{max}] [1 \leq k \leq m]$
	Coagulation integral for a cluster (discrete particle, i -mer) removed from the i^{th} discrete section by coagulation of an i -mer and a k^{th} section agglomerate.	
$\beta_{i,k}^{4ADS}$	$\int_{v_{i-1}}^{v_k} \frac{\theta[i v_m + u < v_k] \beta(i v_m, u) \{ (1 + i v_m / u)^{2/3} - 1 \}}{i v_m (v_k - v_{k-1})} du$	$[1 \leq i \leq i_{max}] [1 \leq k \leq m]$
	Coagulation integral for an agglomerate produced in the k^{th} section by coagulation of a k^{th} section agglomerate and an i -mer.	

The balance of volume in the first section, V_{s1} , is

$$\frac{dV_{s1}}{dt} = \frac{1}{2} \sum_{i=1}^{i_{max}} \sum_{j=1}^{i_{max}} V_{di} V_{dj} \beta_{i,j,1}^{3DD} (i v_m + j v_m) - V_{s1} \sum_{i=1}^{i_{max}} V_{di} \beta_{i,1}^{2DS} + V_{s1} \sum_{i=1}^{i_{max}} V_{di} \beta_{i,1}^{4DS} - \frac{1}{2} V_{s1} V_{s1} \beta_1^{3SS} - V_{s1} \sum_{i=2}^m V_{si} \beta_{i,1}^{4SS} \quad (4)$$

The first RHS term is the production rate of V_{s1} by coagulation of

two discrete particles. The second and third RHS terms are the loss and production rates, respectively, of V_{s1} by discrete particle-agglomerate coagulation. The fourth RHS term is the loss of V_{s1} by coagulation of two first section agglomerates. The last term is the loss of by coagulation of first section agglomerates with larger section agglomerates.

Finally, the balance of volume in the k^{th} section ($k=2$ to m), V_{sk} , is

$$\begin{aligned} \frac{dV_{sk}}{dt} = & \sum_{i=1}^{i_{max}} \sum_{j=1}^{k-1} V_{di} V_{sj} \beta_{i,j,k}^{1DS} + \left[\frac{1}{2} \sum_{i=1}^{k-1} \sum_{j=1}^{k-1} V_{si} V_{sj} (\beta_{i,j,k}^{1SS1} + \beta_{i,j,k}^{1SS2}) \right] \\ & - V_{sk} \sum_{i=1}^{i_{max}} V_{di} \beta_{i,k}^{2DS} - V_{sk} \sum_{i=1}^{k-1} V_{si} \beta_{i,k}^{2SS} + V_{sk} \sum_{i=1}^{i_{max}} V_{di} \beta_{i,k}^{4DS} \\ & + V_{sk} \sum_{i=1}^{k-1} V_{si} \beta_{i,k}^{5SS} - \frac{1}{2} V_{sk} V_{sk} \beta_k^{3SS} - V_{sk} \sum_{i=k+1}^m V_{si} \beta_{i,k}^{4SS} \end{aligned} \quad (5)$$

The first RHS term is the production rate of V_{sk} by coagulation of discrete particles with smaller section agglomerates. The second RHS term is the production rate of V_{sk} by coagulation of two smaller section agglomerates. The third and fourth RHS terms account for the loss of V_{sk} by coagulation of the k^{th} section agglomerates with discrete particles and smaller section agglomerates, respectively. The fifth and sixth RHS terms are the production rate of V_{sk} by coagulation of the k^{th} section agglomerates with discrete particles and smaller section agglomerates, respectively. The seventh RHS term is the loss rate of V_{sk} by coagulation between two k^{th} section agglomerates. The last term is the loss rate of V_{sk} by coagulation of the k^{th} section agglomerates with larger section agglomerates.

2. Surface Area Equations

The discrete particles are assumed to be spherical and the surface area and the diameter of an i -mer (d_{pi}) can be determined simply from the volume (v_{pi}) by $(6v_{pi}/\pi)^{1/3}$. However, the surface area of the particles in a section depends not only on the volume but also on the number of primary particles. In the present model, it is assumed that the number of primary particles composing an agglomerate varies, but the primary particles in a section are of the same size, as shown in Fig. 2.

The volume, v , and the surface area, a , of an agglomerate in the k^{th} section can be represented, respectively, by

$$v = n_{pk} V_{pk} \quad (6)$$

$$a = n_{pk} a_{pk} \quad (7)$$

where n_{pk} is the number of primary-particles in the agglomerate, V_{pk} is the primary-particle volume and a_{pk} is the primary-particle surface area in the k^{th} section.

Similarly, the total volume, V_{sk} , and surface area, A_{sk} , in the k^{th} section are

$$V_{sk} = N_{pk} V_{pk} \quad (8)$$

$$A_{sk} = N_{pk} a_{pk} \quad (9)$$

where N_{pk} is the total number of primary particles in the k^{th} section.

From Eqs. (6), (7), (8) and (9)

$$a = \frac{A_{sk}}{V_{sk}} v \quad (10)$$

By using Eq. (10), the surface area equations were derived in such a way as to share the coagulation integrals calculated for the volume equations. It is demonstrated how the share is possible, for an example: the loss rate of surface area from the k^{th} section by coagulation of k^{th} section particles with smaller section particles. By this coagulation, the rate of surface area change in the k^{th} section can be represented by

$$\left. \frac{dA_{sk}}{dt} \right|_{\beta^{SS}} = \sum_{i=1}^{k-1} \int_{v_{i-1}}^{v_i} \int_{v_{i-1}}^{v_i} \theta[u+v > v_k] \beta(u, v) n(v, t) n(u, t) (a) dv du \quad (11)$$

$\theta[u+v > v_k]$ equals to 1 if $(u+v)$ is greater than, the upper limit of volume section k , and 0, otherwise. $\beta(u, v)$ is the collision coefficient for two agglomerates of volume u in the i^{th} section and v in the k^{th} section, $n(u, t)$ and $n(v, t)$ are the number density functions of the two colliding agglomerates, respectively, and a is the surface area of the agglomerate removed from the k^{th} section by the collision.

The number density functions were assumed to be constant throughout a section as follows [Gelbard et al., 1980]:

$$n(u, t) = \frac{V_{si}}{u(v_i - v_{i-1})} \quad (12)$$

$$n(v, t) = \frac{V_{sk}}{v(v_k - v_{k-1})} \quad (13)$$

By substituting Eqs. (10), (12) and (13) into Eq. (11)

$$\left. \frac{dA_{sk}}{dt} \right|_{\beta^{SS}} = A_{sk} \sum_{i=1}^{k-1} V_{si} \int_{v_{i-1}}^{v_i} \int_{v_{k-1}}^{v_k} \frac{\theta[u+v > v_k] \beta(u, v)}{u(v_i - v_{i-1})(v_k - v_{k-1})} dv du \quad (14)$$

The double integral in Eq. (14) is the same as that of corresponding volume-change equation, $\beta_{i,k}^{2DS}$, in Table 1 of Landgrebe and Pratsinis [1990]. The coagulation integral, $\beta_{i,k}^{2DS}$, calculated for the volume equation can thus be shared by the surface area equation. The proofs of share for the other integrals are shown elsewhere [Moniruzzaman, 2005].

The variation with time of the surface area of particles in the first section, A_{s1} , is represented, using the coagulation integrals calculated for the volume equation, by

$$\begin{aligned} \frac{dA_{s1}}{dt} = & \frac{1}{2} \sum_{i=1}^{i_{max}} \sum_{j=1}^{i_{max}} V_{di} V_{dj} \beta_{i,j,1}^{DD1} [(36\pi)^{1/3} (i v_m + j v_n)^{2/3}] \\ & - A_{s1} \sum_{i=1}^{i_{max}} V_{di} \beta_{i,1}^{2DS} + A_{s1} \sum_{i=1}^{i_{max}} V_{di} \beta_{i,1}^{4DS} - \frac{1}{2} A_{s1} V_{s1} \beta_1^{3SS} \\ & - A_{s1} \sum_{i=2}^m V_{si} \beta_{i,1}^{4SS} - \frac{1}{\tau_1} \left[A_{s1} - V_{s1} \frac{3(36\pi)^{1/3} [v_1^{2/3} - v_0^{2/3}]}{2[v_1 - v_0]} \right] \end{aligned} \quad (15)$$

The first RHS term is the production rate of A_{s1} by coagulation between discrete particles. The second and the third RHS terms are the loss and gain of A_{s1} by coagulation of first section agglomerates with discrete particles. The fourth RHS term is the loss of A_{s1} by coagulation between two first section agglomerates. The fifth RHS term is the loss of A_{s1} by coagulation of first section agglomerates with larger section agglomerates. The sixth RHS term is the loss rate of A_{s1} by sintering of neighboring primary-particles in an agglomerate. The derivation of the sintering term is shown in the appendix.

The balance of surface area in the k^{th} section, A_{sk} , ($k=2$ to m) is

$$\begin{aligned} \frac{dA_{sk}}{dt} = & \sum_{i=1}^{i_{max}} \sum_{j=1}^{k-1} V_{di} A_{sj} \beta_{i,j,k}^{1DS} + \left[\frac{1}{2} \sum_{i=1}^{k-1} \sum_{j=1}^{k-1} A_{si} V_{sj} \beta_{i,j,k}^{1SS1} + \frac{1}{2} \sum_{i=1}^{k-1} \sum_{j=1}^{k-1} A_{sj} V_{si} \beta_{i,j,k}^{1SS2} \right] \\ & - A_{sk} \sum_{i=1}^{i_{max}} V_{di} \beta_{i,k}^{2DS} - A_{sk} \sum_{i=1}^{k-1} V_{si} \beta_{i,k}^{2SS} + A_{sk} \sum_{i=1}^{i_{max}} V_{di} \beta_{i,k}^{4DS} \\ & + V_{sk} \sum_{i=1}^{k-1} A_{si} \beta_{i,k}^{5SS} - \frac{1}{2} A_{sk} V_{sk} \beta_k^{3SS} - A_{sk} \sum_{i=k+1}^m V_{si} \beta_{i,k}^{4SS} \\ & - \frac{1}{\tau_k} \left[A_{sk} - V_{sk} \frac{3(36\pi)^{1/3} [v_k^{2/3} - v_{k-1}^{2/3}]}{2[v_k - v_{k-1}]} \right] \end{aligned} \quad (16)$$

The first RHS term is the production rate by coagulation of smaller section agglomerates with discrete particles. The second RHS term

is the production rate by coagulation between two smaller section agglomerates. The third and fourth RHS terms are the loss rates by coagulation of the k^{th} section agglomerates with discrete particles and smaller section agglomerates, respectively. The fifth and sixth RHS terms are the production rates by coagulation of k^{th} section agglomerates with discrete particles and smaller section agglomerates, respectively. The seventh RHS term is the loss by coagulation between two k^{th} section agglomerates. The eighth RHS term is the loss by coagulation of the k^{th} section agglomerates with larger section agglomerates. The ninth RHS term is the loss rate by sintering.

3. Numerical Method and Simulation Conditions

Eqs. (2), (3), (4), (5), (15) and (16) were solved simultaneously for V_{sk} and A_{sk} by using an ordinary differential-equation solver "ODEINT" [Press et al., 1992]. From the V_{sk} and A_{sk} , the primary particle diameter, d_{pk} , of the k^{th} section was calculated as follows:

$$d_{pk} = 6V_{sk}/A_{sk} \quad (17)$$

The particle number concentration in the k^{th} section, N_{sk} , was determined by the following equation [Landgrebe and Pratsinis, 1990]:

$$N_{sk} = (V_{sk} \Delta v_k) \ln(v_k/v_{k-1}) \quad (18)$$

Details of the FORTRAN code for this model are shown elsewhere [Moniruzzaman, 2005]. The section spacing factor or the ratio of the volume range of a section to that of the section smaller by one unit, f_s , was set at 2.05. The number of discrete sizes, i_{max} , was 20. The number of discrete sizes greater than 18 was reported to be enough [Wu and Flagan, 1988]. With a spacing factor of 2.05, the number of discrete sizes at 20, the molecular volume of TiO_2 at $3.11 \times 10^{-29} \text{ m}^3$ and the upper limit of the last section at $5.23 \times 10^{-19} \text{ m}^3$ in volume or 1,000 nm in diameter for a sphere of equal volume, the number of sections, m , were determined at 29.

The coagulation coefficient, β , for two colliding agglomerates was used as follows [Rogak and Flagan, 1992]:

$$\beta = 2\pi(d_{ci} + d_{cj})(D_i + D_j)f_D \quad (19)$$

where d_{ci} and d_{cj} are the collision diameters, D_i and D_j are the diffusion coefficients for the two agglomerates, and f_D is a correction factor to cover the entire size region from the free molecular to the continuum region [Rogak and Flagan, 1992]. The collision diameter of a spherical particle is its diameter and the collision diameter of an agglomerate composed of primary particles was determined from the equation proposed by Matsoukas and Friedlander [1991], with the mass fractal dimension at 1.8.

For the TiCl_4 oxidation, a first order reaction was assumed with the rate constant as follows [Pratsinis et al., 1990]:

$$k_r = 8.26 \times 10^4 \exp\left(-\frac{88.8(kJ)}{RT}\right) \quad (20)$$

The sintering time for titania used in the surface area equations was obtained from the equation proposed by Kobata et al. [1991].

$$\tau_k = 7.4 \times 10^{16} T d_{pk}^4 \left(\frac{3.1 \times 10^4}{T}\right) \quad (21)$$

where d_{pk} is the primary-particle diameter in the k^{th} section.

The entire time span was divided into a number of time steps. The coagulation integrals and the sintering time were updated every time step by using the primary particle diameter at the previous time

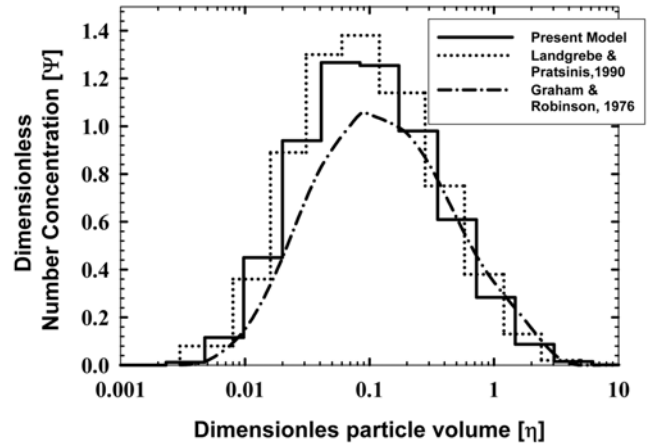


Fig. 3. Comparison of the present model with the v -based model of Landgrebe and Pratsinis [1990] and the 'Normalized Lai's self-preserving distribution of Graham and Robinson [1976] (Simulation conditions are for Fig. 3(a) of Landgrebe and Pratsinis [1990]).

step. The effects of the number of time steps on the accuracy are discussed later.

RESULTS AND DISCUSSION

The present model was compared to the model by Landgrebe and Pratsinis [1990] for a system where a collision between two particles led to a complete coalescence forming a larger spherical particle. This particular case requires the solution of volume equations only since the surface area can be determined simply from the volume. Fig. 3 shows a comparison in particle volume distribution at a residence time long enough to meet the requirement for the self-preserving size distribution. The dimensionless number concentration and the dimensionless particle volume in the figure represent $n(v, t)\bar{v}/N_T$ and v/\bar{v} , respectively, where $n(v, t)$ is the number density function of particles, N_T is the total number concentration and \bar{v} is the number average particle volume. The distribution predicted by the present model is comparable to that of the model by Landgrebe and Pratsinis [1990] but deviates from the precise solution, represented by the solid-dotted curve, of the general dynamic equation given earlier [Graham and Robinson, 1976]. The assumption of the size distribution in a section by a constant value may be a reason for the deviation from the exact size distribution. The deviation was slightly smaller with the present model than with the model by Landgrebe and Pratsinis [1990].

Fractal-like agglomerates, instead of spherical particles, are formed when particle coalescence is slow compared to collision. The primary particles composing an agglomerate then grow by sintering between neighboring primary-particles. In this situation, the volume and surface area equations must be solved simultaneously. The coagulation coefficients for the agglomerates and the sintering time vary with the size of primary particles, as described earlier and are updated every time step by using the primary-particle diameter at the previous time step. The step size would therefore affect the accuracy. The step size was varied from 0.0005 to 0.005 s to study its effect on the average primary particle size, with the TiCl_4 concen-

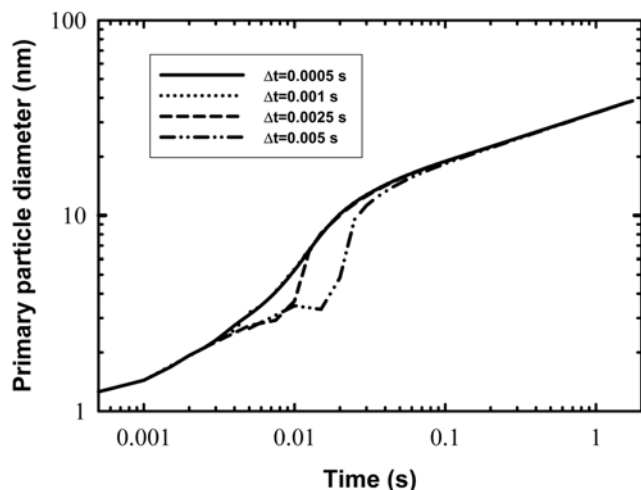


Fig. 4. Effect of time-step size on primary particle size. Δt indicates time-step size (TiCl_4 concentration: 1.35×10^{-5} mol/L; Reactor temperature: 1,300 K).

tration at 1.35×10^{-5} mol/L, the pressure at 1 atm and the reactor temperature at 1,300 K. The result is shown in Fig. 4. Virtually no difference is seen in primary particle diameter between the two step sizes of 0.0005 and 0.001 s. With the step-size increased to 0.0025 s the diameter showed a deviation from those with smaller step sizes, in the range of residence time between 0.002 and 0.01 s. A further increase of the step size to 0.005 s made the deviation persist for a longer period up to the residence time of 0.1 s. At residence times longer than 0.1 s, however, the diameter was insensitive to the step size ranging from 0.0005 to 0.005 s. The computation time must increase with decreasing the step size, and an optimum step size is required to be determined before a simulation is made. The computation time with a personal computer (Pentium IV, 2.8 GHz) was a few hours, varying with simulation conditions.

The sintering law used in the present model was derived for two spheres of equal diameter, and may be effective for the sintering of particles within an agglomerate. The effectiveness of the law may,

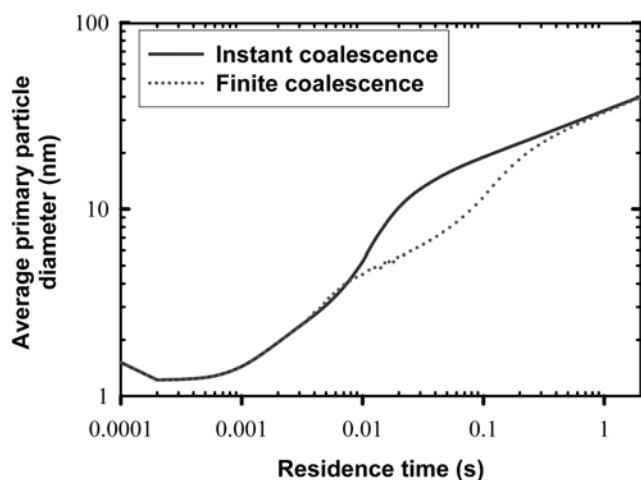


Fig. 5. Comparison of average primary particle size between instantaneous and finite coalescence (TiCl_4 concentration: 1.35×10^{-5} mol/L; Reactor temperature: 1,300 K).

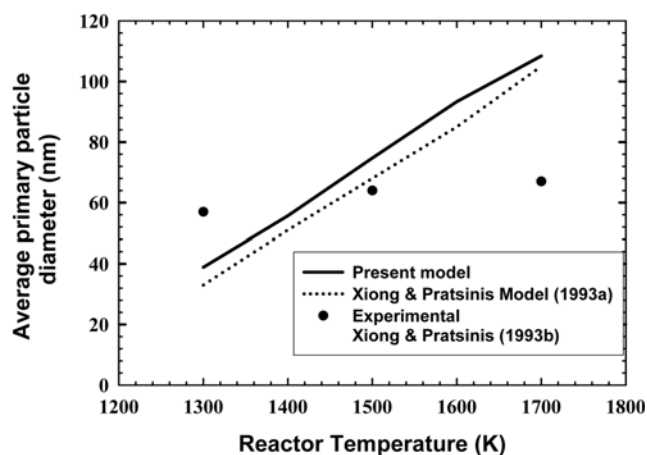


Fig. 6. Comparison of average primary particle size by present model with 2D model and experimental data (TiCl_4 concentration: 1.35×10^{-5} mol/L; Reactor residence time: 1.6 s).

however, be of doubt for a pair differing in size considerably, particularly for a pair resulting from collision of a discrete particle and an agglomerate. The discrete particle is so small that the coalescence may occur instantaneously, rather than at the finite rate calculated by the sintering law. Fig. 5 shows a comparison in primary particle size between the instantaneous and the finite coalescences, at a reactor temperature of 1,300 K and concentration of 1.35×10^{-5} mol/L. In the early stage up to a residence time of about 0.01 s the difference was undetectable, probably because the primary particles were very small and nearly instantaneously coalesced. Thereafter, an appreciable gap in particle size evolved, the particle size being larger with the instantaneous coalescence. After the discrete particles were exhausted, the gap narrowed because of the higher sintering rate of the smaller primary-particles. Eventually, the two sizes became nearly the same at a time of 1.0 s. As the temperature was increased to 1,500 K, the gap was minimal over the whole range of temperature. In the analysis that follows we assume the instantaneous coalescence.

Over a reactor temperature range of 1,300 to 1,700 K, the average primary particle size was compared in Fig. 6 among the present model, the two-dimensional sectional model by Xiong and Pratsinis [1993a] and experimental data [Xiong and Pratsinis, 1993b]. Compared to experimental data the present model underestimated the size at temperatures lower than 1,450 K and overestimated at higher temperatures. The experimental data indicate that the titania sintering rate is not as strong a function of temperature as the theory predicts. The two models gave similar temperature dependency of the size, but the primary particle size obtained by the present model was larger than that of the two dimensional model over the entire range of temperature. The dynamics of small clusters could not be properly accounted for in the 2D model [Xiong and Pratsinis, 1993a]. This may be a reason for the discrepancy between the two models.

Fig. 7 shows the number distributions of the agglomerates varying in size, produced at a temperature of 1,700 K. The agglomerate size is expressed as surface area equivalent diameter, which is defined as the diameter of a sphere whose surface area is the same as the surface area of an agglomerate. The number fraction of the particles in the size range between any two diameters is equal to the area under the curve. As shown in the figure, the surface area equiv-

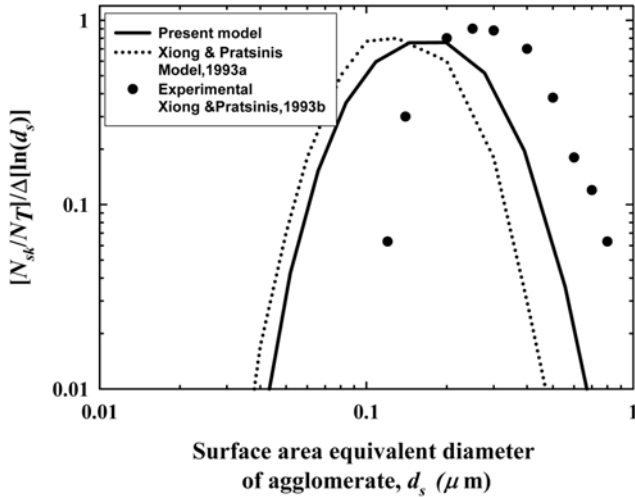


Fig. 7. Comparison of the present model in particle size distribution with experimental data [Xiong and Pratsinis, 1993b] and the model by Xiong and Pratsinis [1993a] (TiCl₄ concentration: 1.35×10⁻⁵ mol/L; Reactor temperature: 1,300 K).

alent diameter was smaller by model prediction. Between two agglomerates of equal volume, the surface area equivalent diameter should be smaller for the agglomerate composed of larger primary particles. This explains why the surface area equivalent diameter predicted by the model was smaller, while the primary particle size, as shown in Fig. 6, was larger than experimental data. The size distribution by the present model is closer to experimental data than that by the 2D model. The inclusion of the discrete regime in the present model may be a reason for the distribution closer to experimental data, compared to the 2D model.

CONCLUSION

A one-dimensional discrete-sectional model for particle growth in aerosol reactors was developed and tested for a production of TiO₂ particles by oxidation of titanium tetrachloride. The present model gave particle size distributions comparable to those by the two-dimensional model which is more rigorous but demands a larger amount of computer time and memory. Compared to experimental data, the primary particle size calculated by the model was more sensitive to the variation of reactor temperature, implying that the activation energy for sintering used in the model may be too high, or an important factor other than the coagulation, condensation and sintering may be missing in the modeling of particle growth. The assumption of instantaneous coalescence for the discrete-particle agglomerate collision led to a significant increase in primary particle size for reactor residence time within a range. Outside the range the instantaneous coalescence had little effect on primary particle size. The present model could not predict experimental data sufficiently and there is an obvious need for improvement, particularly in the particle growth by sintering.

ACKNOWLEDGMENTS

This work was partially supported by grant No. (R 01-2002-000-0004-0) from Korea Science & Engineering Foundation.

APPENDIX: Derivation of the last RHS terms in Eqs. (15) and (16)

The surface area of an agglomerate of volume in the kth section can be given according to Eq. (10)

$$a = \frac{A_{sk}}{V_{sk}} v \tag{A1}$$

The surface area of a completely coalesced sphere having the same volume, v, of the agglomerate is

$$a_s = (36\pi)^{1/3} (v)^{2/3} \tag{A2}$$

The rate of decrease in surface area from an agglomerate of volume v by sintering can be given as [Koch and Friedlander, 1991]

$$\frac{da}{dt} = -\frac{1}{\tau} (a - a_s) \tag{A3}$$

The rate of decrease in surface area by sintering, $dA_{sk}/dt|_{sint}$, for the kth section in the volume range of v_{k-1} to v_k:

$$\left. \frac{dA_{sk}}{dt} \right|_{sint} = - \int_{v_{k-1}}^{v_k} \frac{da}{dt} n(v, t) dv \tag{A4}$$

From Eqs. (A3) and (A4),

$$\left. \frac{dA_{sk}}{dt} \right|_{sint} = - \int_{v_{k-1}}^{v_k} \frac{1}{\tau_k} (a - a_s) n(v, t) dv \tag{A5}$$

From Eqs. (A1), (A2) and (A5),

$$\left. \frac{dA_{sk}}{dt} \right|_{sint} = - \int_{v_{k-1}}^{v_k} \frac{1}{\tau_k} \left[\frac{A_{sk}}{V_{sk}} v - (36\pi)^{1/3} v^{2/3} \right] n(v, t) dv \tag{A6}$$

From Eqs. (13) and (A6),

$$\begin{aligned} \left. \frac{dA_{sk}}{dt} \right|_{sint} &= - \int_{v_{k-1}}^{v_k} \frac{1}{\tau_k} \left[\frac{A_{sk}}{V_{sk}} v - (36\pi)^{1/3} v^{2/3} \right] \left[\frac{V_{sk}}{v(v_k - v_{k-1})} \right] dv \\ &= - \int_{v_{k-1}}^{v_k} \frac{1}{\tau_k} \left[\frac{A_{sk}}{V_{sk}} v \right] \left[\frac{V_{sk}}{v(v_k - v_{k-1})} \right] dv \\ &\quad + \int_{v_{k-1}}^{v_k} \frac{1}{\tau_k} \left[(36\pi)^{1/3} v^{2/3} \right] \left[\frac{V_{sk}}{v(v_k - v_{k-1})} \right] dv \\ &= - A_{sk} \int_{v_{k-1}}^{v_k} \left[\frac{1}{\tau_k (v_k - v_{k-1})} \right] dv + V_{sk} \int_{v_{k-1}}^{v_k} \left[\frac{(36\pi)^{1/3}}{\tau_k v^{1/3} (v_k - v_{k-1})} \right] dv \\ &= - \frac{A_{sk}}{\tau_k} + V_{sk} \frac{3(36\pi)^{1/3} [v_k^{2/3} - v_{k-1}^{2/3}]}{2 \tau_k [v_k - v_{k-1}]} \\ &= - \frac{1}{\tau_k} \left[A_{sk} - V_{sk} \frac{3(36\pi)^{1/3} [v_k^{2/3} - v_{k-1}^{2/3}]}{2 [v_k - v_{k-1}]} \right] \end{aligned} \tag{A8}$$

where [1 ≤ k ≤ m]

NOMENCLATURE

- a : surface area of an agglomerate [m²]
- a_{pk} : primary-particle surface area in the kth section [m²]
- a_s : surface area of a sphere having the volume of an agglomerate [m²]
- A_{sk} : total surface area of all particles in the kth section per unit volume of gas [m² m⁻³]

- c : reactant concentration [molecules m^{-3}]
 D_i : diffusion coefficient for the agglomerate of volume in the i^{th} section [$m^2 s^{-1}$]
 $d_{c,i}$: collision diameter of an agglomerate in the i^{th} section [m]
 $d_{p,k}$: primary-particle diameter in the k^{th} section [m]
 d_s : surface area equivalent diameter of agglomerate [m]
 D_f : mass fractal dimension
 f_D : correction factor given in Eq. (19)
 f_s : section spacing factor
 G : growth rate of particle by condensation [$m^3 s^{-1}$]
 I : nucleation rate of product monomer [molecules m^{-3}]
 i_{max} : maximum number of discrete sections
 k_r : reaction rate constant [s^{-1}]
 m : total number of sections
 n_0 : reaction order
 $n_{p,k}$: number of primary particles in an agglomerate in the k^{th} section
 $N_{p,k}$: total number of primary particles in the k^{th} section per unit volume of gas [m^{-3}]
 $n(u, t)$: size distribution function for particle volume [m^{-6}]
 N_{di} : total number of i -mers per unit volume of gas [m^{-3}]
 N_{sk} : total number of particles in the k^{th} section per unit volume of gas [m^{-3}]
 N_T : total number of particles per unit volume of gas [m^{-3}]
 R : gas constant [$J mol^{-1} K^{-1}$]
 t : time [s]
 T : temperature [K]
 u, v : volume of a particle or in sectional regime [m^3]
 v^* : volume of a critical nucleus [m^3]
 v_m : monomer volume [m^3]
 \bar{v} : number average particle volume [m^3]
 v_{k-1} : lower limit of the particle volume of the k^{th} section [m^3]
 v_k : upper limit of the particle volume of the k^{th} section [m^3]
 $v_{p,i}$: volume of an i -mer [m^3]
 $v_{p,k}$: primary particle volume in the k^{th} section [m^3]
 V_{di} : total volume of all the i -mers per unit volume of gas [$m^3 m^{-3}$]
 V_{sk} : total volume of all particles in the k^{th} section per unit volume of gas [$m^3 m^{-3}$]

Greek Letters

- β : collision frequency function [$m^3 s^{-1}$]
 θ : step function
 τ : characteristic coalescence time [s]
 τ_k : characteristic coalescence time in the k^{th} section [s]
 ψ : dimensionless number concentration [$=n(v, t)\bar{v}/N_T$]
 η : dimensionless particle volume [$=v/\bar{v}$]

REFERENCES

- Friedlander, S. K., *Smoke, dust and haze*, Wiley, New York (1977).
 Gelbard, F. and Seinfeld, J. H., "The general dynamic equation for aerosol;" *J. Colloid Interface Sci.*, **68**, 363 (1979).
 Gelbard, F., Tambour, Y. and Seinfeld, J. H., "Sectional representation for simulating aerosol dynamics;" *J. Colloid Interface Sci.*, **76**, 541 (1980).
 Graham, S. C. and Robinson, A., "A comparison on numerical solutions to the self-preserving distribution for aerosol coagulation in the free-molecular regime;" *J. Aerosol Sci.*, **7**, 261 (1976).
 Jeong, J. I. and Choi, M., "A sectional method for the analysis of growth of polydisperse non-spherical particles undergoing coagulation and coalescence;" *J. Aerosol Sci.*, **32**, 567 (2001).
 Koch, W. and Friedlander, S. K., "The effect of particle coalescence on the surface area of a coagulating aerosol;" *J. Colloid Interface Sci.*, **140**, 419 (1990).
 Kobata, A., Kusakabe, K. and Morooka, S., "Growth and transformation of TiO_2 crystallites in aerosol reactor;" *AIChE J.*, **37**, 347 (1991).
 Landgrebe, J. D. and Pratsinis, S. E., "A discrete-sectional model for particulate production by gas-phase chemical reaction and aerosol coagulation in the free-molecular regime;" *J. Colloid Interface Sci.*, **139**, 63 (1990).
 Matsoukas, T. and Friedlander, S. K., "Dynamics of aerosol agglomerate formation;" *J. Colloid Interface Sci.*, **146**, 495 (1991).
 Moniruzzaman, C. G., *Analysis of iron particle growth by a discrete-sectional model*, MS thesis, 2005, Department of Chemical Engineering, Kongju National University, Chungnam 314-701, Korea.
 Okuyama, K., Kousaka, Y., Tohge, N., Yamamoto, S., Wu, J. J., Flagan, R. C. and Seinfeld, J. H., "Production of ultrafine metal oxide aerosol particles by thermal decomposition of metal alkoxide vapors;" *AIChE J.*, **32**, 2010 (1986).
 Pratsinis, S. E., Bai, H., Biswas, P., Frenklach, M. and Mastrangelo, S. V. R., "Kinetics of titanium (IV) chloride oxidation;" *J. Am. Ceram. Soc.*, **73**, 2158 (1990).
 Press, W. H., Teukolsky, S. A., Vetterling, W. T. and Flannery, B. P., *Numerical recipes in FORTRAN 77*, Cambridge University Press (1992).
 Rogak, S. N. and Flagan, R. C., "Coagulation of aerosol agglomerates in the transition regime;" *J. Colloid Interface Sci.*, **151**, 203 (1992).
 Tsantilis, S. and Pratsinis, S. E., "Evolution of primary and aggregate particle-size distribution by coagulation and sintering;" *AIChE J.*, **46**, 407 (2000).
 Ulrich, G. D., "Theory of particle formation and growth in oxide synthesis flames;" *Combust. Sci. Technol.*, **4**, 47 (1971).
 Wu, J. J. and Flagan, R. C., "A discrete-sectional solution to the aerosol dynamic equation;" *J. Colloid Interface Sci.*, **123**, 339 (1988).
 Xiong, Y. and Pratsinis, S. E., "Formation of agglomerate particles by coagulation and sintering-part I. A two-dimensional solution of the population balance equation;" *J. Aerosol Sci.*, **24**, 283 (1993a).
 Xiong, Y. and Pratsinis, S. E., "Formation of agglomerate particles by coagulation and sintering-part II. The evolution of the morphology of aerosol-made titania, silica and silica-doped titania powders;" *J. Aerosol Sci.*, **24**, 301 (1993b).